Published in final edited form as:
J Comp Neurol. 2006 January 10; 494(2): 358–367. doi:10.1002/cne.20814.

Cytoskeletal Organization of the Developing Mouse Olfactory Nerve Layer

Michael R. Akins[1] and **Charles A. Greer**[1,2,3]

[1]Interdepartmental Neuroscience Graduate Program, Yale University School of Medicine, New Haven, Connecticut 06520

[2]Department of Neurosurgery, Yale University School of Medicine, New Haven, Connecticut 06520

[3]Department of Neurobiology, Yale University School of Medicine, New Haven, Connecticut 06520

Abstract

Olfactory sensory neuron (OSN) axonal extension and targeting occurs within the olfactory nerve layer (ONL) of the olfactory bulb (OB). The ONL can be differentiated into sublaminae: the outer (ONLo), where axons broadly target regions of the OB in tight fascicles, and inner (ONLi), where axons perform final targeting in loosely organized fascicles. During perinatal development cadherin-2 and its binding partner, gamma-catenin, are preferentially expressed by OSN axons in the ONLo versus the ONLi. Given the expression of these cytoskeletal associated molecules, we hypothesized that cytoskeletal elements of OSN axons may be differentially expressed across the ONL. We therefore examined cytoskeletal organization of OSN axons in the ONL, focusing on the day of birth (P0). We show that microfilaments, microtubules, and the intermediate filament (IF) vimentin are homogeneously expressed across the ONL at P0. In contrast, the IFs peripherin and alpha-internexin are preferentially localized to the ONLo at P0, with alpha-internexin expressed by a restricted subset of OSNs. We also show that OSN axons in the ONLo are significantly smaller than those in the ONLi. The data demonstrate that as OSN axons begin to exit the ONLo and target a specific region of the OB there is a down-regulation of cytoskeletal elements and bound extracellular adhesion molecules. The increase in axon diameter may reflect additional mechanisms involved in glomerular targeting or the formation of the large terminal boutons of OSN axons within glomeruli.

Keywords

peripherin; α-internexin; vimentin; actin; phalloidin; tubulin; cadherin; γ-catenin; plakoglobin; olfaction; olfactory sensory neuron

INTRODUCTION

Olfactory sensory neuron (OSN) axons exit the olfactory epithelium (OE) and coalesce to form the olfactory nerve (ON) before projecting to the olfactory bulb (OB), the rostralmost extension of the telencephalon and first site of olfactory processing. Upon reaching the OB, OSN axons form a plexus, the olfactory nerve layer (ONL). Within the ONL, axons reorganize extensively before reaching their target glomerulus (Au et al., 2002; Treloar et

Correspondence to: Charles A. Greer, Department of Neurosurgery, Yale University School of Medicine, 333 Cedar Street, P.O. Box 208082, New Haven, CT 06520-8082; charles.greer@yale.edu.

al., 2002; Akins and Greer, 2005), a region of neuropil that serves as the fundamental olfactory processing unit. Each glomerulus receives input from OSNs expressing the same odorant receptor (OR) (Ressler et al., 1994; Vassar et al., 1994; Mombaerts et al., 1996; Treloar et al., 2002), which maintains the molecular specifity of odor responses from the level of the OSN to the glomeruli (Zhao et al., 1998; Malnic et al., 1999). Correct targeting to a specific glomerulus by each OSN axon is thus fundamental to the olfactory system's ability to discriminate odorants.

OSN axon targeting appears to occur in at least two phases—gross targeting, which directs the axons to a general region of the OB and occurs in the outermost ONL (ONLo), and fine targeting, which includes the innervation/formation of a specific glomerulus and occurs from within the inner ONL (ONLi) (Au et al., 2002; Treloar et al., 2002; Akins and Greer, 2005). Within the ONLo, axons are tightly bundled with little reorganization. When they approach their target region of the OB they enter the ONLi, become more loosely fasciculated and exhibit highly complex trajectories as they reorganize into subsets of axons that are defined by odor receptor expression (Au et al., 2002; Treloar et al., 2002; Akins and Greer, 2005). Differences in axonal bundling and trajectories may reflect interactions with subpopulations of molecularly differentiated olfactory ensheathing cells (OECs), specialized glia found in the ONL (Au et al., 2002; Hisaoka et al., 2004). In addition, during perinatal development the expression of the cellular adhesion molecule neuronal-cadherin (CDH2, N-cadherin) and one of its intracellular binding partners, γ-catenin, differs across the ONL (Akins and Greer, 2005). We have speculated that these changes in cadherin expression may underlie the different roles of axon extension versus glomerular targeting that we ascribe to the ONLo and the ONLi, respectively.

Axons respond to cues in the extracellular milieu through alterations in their cytoskeleton. In particular, actin and microtubules are major components of axons and axonal growth cones and are required for directed axonal growth (Marsh and Letourneau, 1984; Chien et al., 1993; Williamson et al., 1996; Challacombe et al., 1997). Intermediate filaments (IFs) are also localized to at least some growth cones, and the IFs α-internexin and peripherin are required *in vitro* for neurite outgrowth (Shea and Beermann, 1999; Helfand et al., 2003) and *in vivo* for axon sprouting following injury (Belecky-Adams et al., 2003). Given the roles of the cytoskeleton in axon behavior and the differential expression of the cytoskeleton associated proteins CDH2 and γ-catenin between the ONLo and ONLi (Akins and Greer, 2005), it is plausible that differences in axonal bundling and trajectories between the ONLo and ONLi may reflect differences in cytoskeletal organization.

To pursue this hypothesis we examined the expression of cytoskeletal components in OSN axons in the ONLo and ONLi sublaminae. The expression of microtubules, and the IFs vimentin, peripherin, and α-internexin have been established in OSN axons, but sublaminar organization within the ONL has not been examined (Schwob et al., 1986; Gorham et al., 1991; Chien et al., 1998; Burton and Paige, 1981). Our data demonstrate a differential localization of cytoskeletal elements in OSN axons in the ONLo versus the ONLi. Consistent with a change in cytoskeletal organization, we also report significant differences in the diameter of OSN axons in the two sublaminae of the ONL. These differences declined as the system matured and glomerulogenesis was completed suggesting that the expression of the cadherin complex and axonal intermediate filaments may be especially important during initial formation of the glomerular map, but less so in the mature system..

METHODS

Animals

Pregnant, time-mated CD-1 mice (Charles River, Wilmington, MA) were anesthetized with sodium pentobarbital (80 mg/kg, i.p.; Nembutal; Abbott laboratories, Chicago, IL) prior to cesarean section. The embryos were immersion-fixed in 4% paraformaldehyde (PFA) in phosphate-buffered saline (PBS; 0.1 M phosphate buffer and 0.9% NaCl, pH 7.4) at 4°C overnight. Embryos were collected at embryonic day (E) E15, where the day of conception is designated E0. Postnatal (P) mice at P0 (day of birth) and P7 were rapidly decapitated and immersion fixed in 4% PFA in PBS at 4°C overnight. For adult tissue, adult CD1 mice were anesthetized with 80 mg/kg Nembutal and perfused with 4% paraformaldehyde in 0.1 M phosphate buffered + 0.9% saline (PBS; pH 7.4). The brains were removed, and the OBs were dissected out and immersed in the fixative overnight at 4°C. All tissue was rinsed for a minimum of 2 hrs in PBS after fixation before processing for microscopy. The procedures for preparing tissue for electron microscopy are described below. All procedures undertaken in this study were approved by Yale's Animal Care and Use Committee and conform to NIH guidelines.

Sectioning

Tissue was cryoprotected by immersion in 30% sucrose in PBS at 4°C until tissue sank. Tissue was embedded in OCT compound (Sakura Finetek, Torrance, CA) and frozen in a slurry of 100% ethanol and dry ice. The tissue was then serially sectioned in the coronal or sagittal plane (20 μm thick) using a Reichert-Jung 2800 Frigocut E cryostat. Sections were thaw mounted onto SuperFrost Plus microscope slides (Fisher Scientific, Pittsburgh, PA), air dried, and stored at -20°C until needed.

Immunohistochemistry

The 20 μm cryostat sections were incubated with Alexa-conjugated phalloidin (Molecular Probes, Eugene, OR; 1:200) and/or immunostained with antibodies (Table 1) ($n \geq 3$ for each condition). Briefly, tissue was thawed, air dried, and exposed for 10 min to vapor from 0.01 M sodium citrate in a commercial steamer (excepting sections labeled with phalloidin). The tissue was then incubated with 2% bovine serum albumin (BSA) (Sigma) in TBST [0.1 M Tris buffer and 0.9% saline, pH 7.4 (TBS), with 0.3% Triton X-100 (Sigma)] for 30 min to block nonspecific binding sites. Incubation in primary antibodies in blocking solution was overnight at room temperature. Sections were washed three times in TBST for 5 min and incubated in secondary antibodies or avidin (in the case of DBA) conjugated to Alexa Fluors (Molecular Probes) diluted 1:1000 in blocking buffer for 1 hr at room temperature. Sections were washed (as above), rinsed in TBS, mounted in Gel/Mount mounting medium (Biomeda Corp, Foster City, CA), and coverslipped. Omission of the primary antibody was used to establish the specificity of staining. Antibodies employed as tissue markers exhibited staining patterns consistent with previous reports. Stained sections were analyzed using a Bio-Rad MRC-600 laser scanning confocal microscope. Digital images were collected from a single optical plane, ~1 μm thick.

Electron Microscopy

The general protocols we employ for preparing tissue for electron microscopy have been previously described (Kasowski et al., 1999; Au et al., 2002). Briefly, adult CD1 mice ($n = 2$; Charles River, Wilmington, MA) were anesthetized with 80 mg/kg of sodium pentobarbital (Nembutal) and perfused with PBS [0.1M phosphate buffer (PB), 0.9% NaCl, pH 7.4] followed by 4% paraformaldehyde and 2% glutaraldehyde in PBS. The brains were left *in situ* at 4°C for 1 hr after which the OBs were removed and post-fixed overnight at

4°C. CD1 mice at P0 (n = 2) were decapitated and the brains immersion fixed in 2% glutaraldehyde with 0.2% tannic acid in 0.1M PB. The OBs were cut coronally at 100μm in a vibratome (Pelco series 1000) and then washed 3X for 10 min each in PBS prior to osmication with 2% osmium tetrachloride for 1 hr. Following a series of graded alcohol washes the sections from the adult mice were stained *en bloc* with 1% uranyl acetate in 70% EtOH for 1 hr, while those from the P0 mice were stained *en bloc* with 1% uranyl acetate in water. Following an overnight immersion in a 1:1 mix of propylene oxide and Epon 812 (Epon), the sections were infiltrated with fresh Epon for 2 hrs, flat embedded in fresh Epon onto quick-release-coated slides (Hobby Time Mold Parting Compound; Electron Microscopy Sciences, Ft. Washington, PA), coverslipped with quick-release-coated coverslips, and polymerized in a 60°C oven. Slides were examined with a light microscope, and areas of the Epon film containing OB tissue with intact ONL on the medial wall of the OB were cut out and remounted on Epon blocks and polymerized for 48 hours prior to thin sectioning. Silver sections (70-100nm) were cut with a Reichert-Jung Ultramicrotome, mounted on slotted grids (2mm X 1mm) which were then post-stained with 1% lead citrate for 1.5 min, and examined using a JEOL 1200 EXII 120kV transmission electron microscope (Peabody, MA).

Electron micrographs were captured at a primary magnification of 3,000X and 6,000X, with final working magnifications of 7,500X and 15,000X after printing. The individual electron photomicrographs were combined to make a montage that spanned the entire thickness of the ONL and proximal portions of the GL in cross section.

Measuring Axon Diameters

OSN axons are readily identified ultrastructurally in the ONL (Au et al., 2002). OSN axon profiles randomly selected from electron micrographs from the ONLo and ONLi were measured for cross-sectional diameter (56 in each sublamina and age; total of 224). Axons cut obliquely were not included. Longitudinal axons were measured for their shortest diameter at a randomly selected point along the axon. Because axons increase their diameter around mitochondria and form a varicosity, axon profiles containing mitochondria were not included in the analysis. A 2-way ANOVA (ONL lamina X age) was used to test for differences in axon diameter.

Riboprobes

Riboprobe labeled with digoxigenin-11-UTP (Roche Diagnostics, Indianapolis, IN) against α-internexin was made against the full length mouse sequence (Clone 4502421 from Invitrogen, Carlsbad, CA) using a MEGAscript kit (Ambion Inc, Austin, TX) as per the directions in the kit.

In situ Hybridization

1st day—Solutions used on the first day were made in water treated with diethyl pyrocarbonate (DEPC). Sections were thawed and dried at 37° for 15 min. Tissue was then immersed in phosphate buffered saline (DEPC-PBS; 0.1 M Phosphate buffer, 0.9% saline, pH 7.4) for 1 min, followed by a 10 minute immersion in 0.2 M HCl. Tissue was immersed in 1% Triton X-100 in DEPC-PBS for 2 min, followed by two 1 min washes in DEPC-PBS. Tissue was treated with 50% formamide/5X SSC (1X SSC = 15 mM Sodium Citrate, 150 mM Sodium Chloride, pH 7.0) for 10 min. Sections were incubated in the appropriate probe at 1 ng/μL in hybridization solution [50% formamide, 10mM Tris (pH 8.0), 200 μg/mL yeast tRNA, 10% dextran sulfate, 1X Denhardt's Solution, 600 mM sodium chloride, 0.25% SDS, 1 mM EDTA] overnight at 65° C.

2nd day—Tissue was washed twice in 0.1X SSC at 65° for 30 min each time. Following steps take place at room temperature. Sections were incubated in block [1% blocking reagent (Roche Diagnostics) in TBST] for 30 min, followed by a one hour incubation in a polyclonal antibody against digoxigenin conjugated to alkaline phosphatase (Roche Diagnostics) in block. Sections were washed three times for five min each in TBS + 0.1% Triton X-100, followed by a rinse in AP buffer [100 mM Tris (pH 9.5), 100 mM Sodium Chloride, 5 mM Magnesium Chloride]. Tissue was incubated in NBT/BCIP (Roche Diagnostics) diluted 1:50 in AP buffer for one hr. Tissue was rinsed in AP buffer and incubated in NBT/BCIP in AP buffer overnight.

3rd day—Tissue was rinsed in distilled water to stop the development reaction, before soaking in methanol for ten min. Tissue was mounted with Crystal/Mount mounting medium (Biomeda Corp). Digital images were collected using an Olympus Magnafire camera attached to an Olympus BX51 microscope.

Camera Lucida

Sections processed for *in situ* hybridization were examined on an Olympus BH-2 microscope equipped with a camera lucida. Images were drawn at 4X. These images were digitized by tracing on an Intuos Graphics Tablet (Wacom, Vancouver, WA) using Corel Draw 12.0 (Corel, Ottawa, Ontario, Canada).

Image Preparation

All digital images were color balanced using Adobe Photoshop 6.0 (Adobe Systems, San Jose, CA). The composition of the images was not altered in any way. Plates were constructed using Corel Draw 12.0 (Corel).

RESULTS

Cytoskeletal Organization in the ONL

To assess the organization of the cytoskeleton in the ONL, we stained P0 OBs with phalloidin (to visualize the localization of f-actin) and antibodies to α-tubulin (to assess microtubule location) and the IFs vimentin, α-internexin, and peripherin (Figures 1,2). The ONL can be divided into an ONLo (growth zone) and ONLi (sorting zone), based in part on OSN axon expression of CDH2 and γ-catenin (Akins and Greer, 2005). Expression levels of each are higher in the ONLo than in the ONLi at P0. To differentiate between the ONLo and ONLi at P0, we double-labeled sections with γ-catenin; the border between the ONLo and ONLi defined by γ-catenin is indicated with a dotted line (Figures 1, 2).

To assess localization of the f-actin cytoskeleton at P0, phalloidin (green; Figure 1A,B) staining was combined with immunofluorescence for γ-catenin (red; Figure 1B,C). Phalloidin did not exhibit any differential expression across the ONLo and ONLi border established by the γ-catenin staining. The most intense staining for phalloidin was present in glomeruli, possibly reflecting the density of synapses in this neuropil (Toh et al., 1978; Kasowski et al., 1999; Rossler et al., 2002).

To assess the distribution of the microtubule cytoskeleton, we double-labeled P0 sections for α-tubulin (green; Figure 1D,E) and γ-catenin (red; Figure 1E,F). Staining was widespread and did not show specificity for any of the OB laminae. In particular, expression intensity was uniform across the ONL. Equivalent results were obtained for β-tubulin (data not shown).

To visualize vimentin localization, we double-labeled P0 sections for vimentin (green; Figure 1E,F) and γ-catenin (red; Figure 1F). Staining was widespread and included nonneuronal tissue, including blood vessels (arrow in Figure 1E,F). Expression was uniform across the ONLo, ONLi, and glomerular layer.

To localize the IF α-internexin at P0, we double-labeled sections with α-internexin (green; Figure 2A,B) and γ-catenin (red; Figure 2B,C). At P0, α-internexin was expressed by subsets of OSN axons in the ONLo (Figure 2A,B) as well as dendrites of OB neurons (arrow, Figure 2A,B) and some blood vessels. The selective expression of α-internexin in a subset of fascicles of the ON as it entered the ONL was of particular interest. As shown in Figure 2A-C the fascicle indicated by the arrowhead did not express α-internexin, although it was positive for the OSN axon marker γ-catenin (Fig. 2B,C) (and NCAM; data not shown). Expression at E15 and P7 was similar to that described for P0. In the adult there was no evidence of α-internexin expression in OSN axons (data not shown).

To localize the IF peripherin we double-labeled sections with peripherin (green; Figure 2D,E,G,H) and γ-catenin (red; Figure 2E,F,H,I). At P0, peripherin was expressed by OSN axons within the ONLo while it down-regulated or was absent from the ONLi. Unlike α-internexin, peripherin was expressed uniformly around the OB and was present in all fascicles examined. CDH2 and γ-catenin are expressed more strongly by OSN axons in the ONLo at P0, but are uniformly expressed across the ONL surrounding the majority of the OB at P7 (Akins and Greer, 2005). Peripherin expression was evident across the ONL at P7, albeit more strongly in the ONLo than ONLi (Figure 2G,H). Furthermore, peripherin was expressed heterogeneously within the ONLi, perhaps reflecting expression by only a subset of OSN axons (Figure 2G,H; inset from 2H shown in 2I) (Gorham et al., 1991). Peripherin relocalization appeared to lag behind that seen for CDH2 and γ-catenin; at P7 the peripherin ONLo/ONLi border was still evident across much of the OB while γ-catenin staining was uniform across the ONL. In the adult mouse peripherin expression was uniform across the ONL with no evident border between the ONLo and ONLi (data not shown).

α-Internexin Expression by Spatially Restricted Sensory Neurons

Because α-internexin antibody staining was restricted to the axons of OSNs, *in situ* hybridizations were used to assess the distribution of α-internexin$^+$ cells in the OE. Sections from both E15 and P0 mice demonstrated similar staining patterns. α-Internexin was expressed by OSNs within the supralateral and ventromedial nasal cavity (Figure 3A,B). Regions reactive for α-internexin are highlighted in black on the right half of Figure 3A. Closer examination of the dorsolateral portion of the OE shows a sharp border of α-internexin expression (arrows in Figure 3B). The α-internexin positive OSNs were typically restricted to the basal portion of OE (Figure 3C).

In addition to expression in the main OE, α-internexin expression was also observed in two other olfactory organs—the septal organ (SO) of Masera (Figure 3A,D) and the vomeronasal organ (VNO) (Figure 3E). Expression in the SO was evident in the basal portion of the epithelium (Figure 3D), as was seen for the main OE. α-Internexin was also expressed in a subset of sensory neurons in the basal portion of the VNO epithelium (Figure 3E).

The *in situ* hybridization localization at E15 and P0, as well as the complementary protein expression at E15, P0, and P7, led us to conclude that α-internexin was expressed by a similar cohort of cells at all perinatal ages. We thus focused further study on P0, when the structure of the OE is defined and α-internexin expression is still widespread. To determine if α-internexin was expressed in patches or continuously along the OE, we performed *in situ* hybridization for α-internexin on serial sections from a P0 mouse. Camera lucida drawings of these sections are summarized in Figure 4 and suggest that clusters of OSNs in the OE

express α-internexin, but that these do not necessarily occur in a contiguous pattern. Beginning at the rostral portion of the OE, α-internexin expression was first observed ventrally on the nasal septum. As lateral turbinates appeared, expression was also observed dorsolaterally. Caudally, these medial and lateral regions merged into ventral expression. By comparing the total length of OE in these sections with the length that contain OSNs expressing α-internexin, we estimate that ~35% of the OE contained α-internexin positive OSNs. In sections from 400 to 700 μms caudal to the rostral pole of the OE, the SO expressed α-internexin along its entire rostrocaudal axis. Finally, α-internexin was expressed throughout the rostrocaudal axis of the VNO.

OSN Axon Diameters

Because cytoskeletal organization can be an important determinant of cell shape, we next examined whether the diameters of OSN axons exhibited any variation across the ONLo and ONLi. Using electron micrographs of the ONL from P0 and adult animals (Figure 5), we quantified axon diameters in 56 randomly selected axons from each of the ONL sublaminae at each age. Axons within the ONLo (Figure 5A,C,E) at both ages were the smallest, approximately 0.2 μm, consistent with earlier characterizations of the mouse olfactory nerve (Cuschieri and Bannister, 1975). Within the ONLi, axon diameter increased, with a greater difference seen at P0 (Figure 5B,D) than in the adult (Figure 5F). Longitudinal views of P0 axons in the ONLo (Figure 5C) and ONLi (Figure 5D) demonstrate that these diameters are consistent for long portions of the axons and do not arise from an increase in axonal varicosities within the ONLi. Axon diameters (± SEM) were as follows: P0 ONLo—0.2438 ± 0.01 μm; P0 ONLi—0.4439 ± 0.02 μm; adult ONLo—0.2355 ± 0.01 μm; adult ONLi—0.343 ± 0.02 μm. A two way ANOVA confirmed a statistically significant age effect ($p<0.01$), laminae effect ($p<0.01$), as well as an interaction between age and laminae ($p<0.01$).

DISCUSSION

The data reported here provide several lines of evidence consistent with the hypothesis that IFs contribute to the organization of OSN axons during olfactory development. First, the IFs peripherin and α-internexin localize within the mouse ONL in distinct spatio-temporal patterns that correlate with the spatial organization of OSN axons, their expression of cytoskeletal-linked cell surface adhesion molecules and with glomerulogenesis. Second, spatio-temporal expression patterns of cytoskeletal elements is not ubiquitous; vimentin and elements of the microtubule cytoskeletal network in OSN axons were homogeneously expressed. Phalloidin staining was evident, in contrast to earlier reports (Rossler et al., 2002), although no differences were found in ONL expression. Third, paralleling the molecular changes in OSN axons is a significant increase in cross-sectional diameter of OSN axons in the ONLi versus the ONLo.

Sublaminar Expression of Intermediate Filaments

IFs within OSNs are differentially distributed among subcellular compartments. In the adult, vimentin is found throughout the cell, though largely excluded from glomerular processes (Schwob et al., 1986; Gorham et al., 1991), while peripherin is excluded from dendrites, somata, and glomerular terminals (Gorham et al., 1991). Our new findings show that peripherin and α-internexin are excluded from the ONLi during a pivotal perinatal period. At least two possibilities could explain this restricted expression within axons. First, IFs may be expressed only by immature axons and downregulated as the growth cone enters a new lamina. Alternatively, IF proteins may be maintained within axonal subcompartments with local expression changing as axons pass through different extracellular environments. Expression exclusively by immature OSNs, seems less likely since the ONL is a matrix of

both immature and mature OSN axons throughout life (Graziadei and Graziadei, 1979; Verhaagen et al., 1989). We favor the interpretation that peripherin and α-internexin are restricted within an axonal subcompartment. Such a restriction has been seen for adhesion molecules (Bastiani et al, 1987; Dodd et al, 1988), which may arise from local protein synthesis (Brittis et al, 2002). Further, as noted above, IFs are restricted from OSN axons in glomeruli (Schwob et al., 1986; Gorham et al., 1991).

Potential Roles of Intermediate Filaments

IFs can provide structural integrity to a cell (Lloyd et al., 1995; Wong et al., 2000; Fuchs and Cleveland, 1998; Yamasaki et al., 1991; Ohara et al., 1993; Eyer and Peterson, 1994; Zhu et al., 1997) due at least in part to the relative physical strength of IFs in comparison to microfilaments and microtubules (Beil et al., 2003; Janmey et al., 1991; Ma et al., 2001; Yamada et al., 2002). However, a role in maintaining cellular integrity is not consistent with the developmental changes seen in subcellular localization of peripherin or with zonal expression of α-internexin during a restricted developmental window. Another role for IFs more consistent with the expression patterns seen in the developing olfactory system is regulation of the subcellular localization of other proteins, and thereby affecting cellular signaling (Runembert et al., 2002; Sin et al., 1998; Tzivion et al., 2000; Gilbert et al., 2001; Inada et al., 2001; Ameen et al., 2001; Toivola et al., 2004). While peripherin and α-internexin have not had such roles ascribed specifically to them, it seems likely that IFs in general play a role in protein localization.

The differential expression of IFs within OSN axons effectively produces two distinct subcellular compartments. These two compartments could underlie differing axonal responses within the two sublaminae in the ONL. Within the ONLo, the receptors and effectors that guide gross targeting could be held in close proximity, while the receptors and effectors that guide sorting would be kept apart. Within the ONLi, in the absence of IFs, the situation would be reversed, and receptor/effector combinations that are responsible for axonal sorting would be allowed to interact. One possibility is that the OR proteins themselves, which are known to have a role in axonal sorting into glomeruli (Feinstein et al., 2004; Feinstein and Mombaerts, 2004), would be sequestered from their effectors within the ONLo. This would be consistent with evidence that the ORs are important for fine targeting and the proposal that ORs interact with other proteins during targeting (Mombaerts et al., 1996; Wang et al., 1998; Feinstein et al., 2004; Feinstein and Mombaerts, 2004).

Axons within the ONLo and ONLi are structurally different. Axons in the ONLi have a larger diameter than those in the ONLo, particularly in the P0 mice. Our data are consistent with and extend evidence from Golgi stains in the rabbit and electron microscopy in frog (Burton, 1987) that individual axons increase in diameter as they approach their target glomeruli (Yilmazer-Hanke et al., 2000). The current report is the first, however, to recognize that the change in diameter occurs in conjunction with a shift in axons from the ONLo to the ONLi. Peripherin expression correlates with small axonal diameter elsewhere, such as spinal cord dorsal roots (Goldstein et al., 1991). Our results are consistent with these reports and suggest that peripherin may serve to limit axonal caliber in the ONLo as axons exhibit rapid growth. When axons enter the ONLo to sort, peripherin is downregulated and axonal caliber increases. This increase in diameter may provide for a greater surface area for receptor insertion and increased interaction with and sampling of the environment by the axon.

A Link between Intermediate Filaments and Cadherins?

We previously described the cadherin CDH2 and its associated protein, γ-catenin, as heavily localized to the ONLo during perinatal development before becoming uniform across the

ONL as development proceeds (Akins and Greer, 2005). In this paper, we demonstrate that peripherin and α-internexin expression is limited to the ONLo during development. These data suggest that IFs and cadherin-mediated adhesion may work in concert to affect OSN axon targeting.

Are cadherins and IFs interacting or merely influencing the same process? Cadherins normally interact with the actin cytoskeleton through α-catenin. However, we have previously shown that CDH2 and γ-catenin, but not α-catenin, are localized in the same pattern as peripherin. Interestingly CDH5 (VE-cadherin) associates with the IF vimentin through γ-catenin and desmoplakin, a member of the plakin family of cytoskeletal linkers (Valiron et al., 1996; Kowalczyk et al., 1998). Whether a member of the plakin family, or a related molecule, that could serve as a bridge between γ-catenin and the IFs is expressed within OSN axons remains to be determined.

Expression of α-Internexin by Immature Neurons

α-Internexin is expressed early in neuronal differentiation (Kaplan et al., 1990; Fliegner et al., 1994) and is generally replaced by other neurofilaments in mature neurons. Within OSN axons, however, no other neurofilaments are expressed (Chien et al., 1998). α-Internexin may instead give way to a peripherin/vimentin IF cytoskeleton, as is seen in OSNs originating from other portions of the OE. α-Internexin protein within OSNs is restricted from the somatodendritic compartment into the axon. It thus seems unlikely that it is playing a role strictly in epithelial development. Rather, α-internexin is more likely regulating axon elongation or guidance. While axonal elongation is unperturbed in mice lacking α-internexin (Levavasseur et al., 1999), studies using antisense oligonucleotides or blocking antibodies demonstrate a role for α-internexin in cellular polarization, neurite outgrowth, and stabilization of the microtubule cytoskeleton (Shea and Beermann, 1999). α-Internexin may thus be conferring a specific response within immature OSNs originating from a spatially restricted portion of the OE. It seems plausible that this may include events such as axon guidance and/or extension cues, by changing the organization of the IF cytoskeleton and thereby altering cellular responses, perhaps by regulating cadherin based adhesion.

In the VNO the apical and basal sensory neurons are differentiated based on expression of different families of vomeronasal receptors, adhesion molecules, and signal transduction elements. In parallel with these molecular differences, apical VNO sensory neurons project to the rostral AOB while basal VNO neurons project to the caudal AOB (Dulac and Axel, 1995; Halpern et al., 1995; Berghard and Buck, 1996; Herrada and Dulac, 1997; Matsunami and Buck, 1997; Ryba and Tirindelli, 1997; von Campenhausen et al., 1997). The selective expression of α-internexin in the basal VNO could reflect expression by the subset of neurons that project selectively to the caudal AOB. Alternatively, since immature neurons first appear deep in the epithelium and then migrate to their final positions as they differentiate and mature (Cappello et al, 1999; Giacobini et al, 2000; Martinez-Marcos et al, 2005), the selective expression of α-internexin in the deep or basal VNO epithelium could suggest a selective expression by immature neurons that have not yet differentiated into basal versus apical subpopulations. The restriction of α-internexin to the outer vomeronasal nerve layer (our unpublished observations) precluded distinguishing between these possibilities. However, we did not note a segregation of α-internexin expressing axons in the vomeronasal nerve (our unpublished observations), which would seem to favor the former interpretation.

Zonal Expression of α-Internexin

The expression of α-internexin in a spatio-temporally restricted fashion suggests that it is involved in establishment of the olfactory map, but not its maintenance. Indeed, α-

internexin expression correlates with zone 4 of the OE (Mori et al., 1999), indicating a potential role in map establishment. α-Internexin might, as discussed above, serve to localize a receptor or effector in a different manner than that seen in OSNs in the remainder of the OE. This differential interaction could underlie the targeting of zone 4 axons to the ventral OB during the period of glomerulogenesis. At the conclusion of initial glomerular formation, when α-internexin expression is lost, different cues, such as homophilic adhesion of axons expressing the same OR, would be responsible for axon targeting. This is consistent with the hypothesis that axonal targeting in the developing olfactory system is fundamentally different from that seen in the adult, as seen by the failure of the olfactory system to properly regenerate after lesion (Schwob et al., 1999; St.John and Key, 2003).

OSNs residing in three different regions express α-internexin—zone 4 of the main OE, the SO, and the VNO. The SO axons target the main OB (Ma et al., 2003; Tian and Ma, 2004) while the sensory neurons of the VNO target the AOB. Zone 4 and the SO project axons to similar locations (Astic and Saucier, 1988; Astic et al., 1987; Astic and Saucier, 1986; Giannetti et al., 1992; Saucier and Astic, 1986) and appear developmentally related (Astic and Saucier, 1988; Giannetti et al., 1995). Furthermore, they express a similar cohort of ORs (Tian and Ma, 2004). Thus, the SO appears to be a highly specialized derivative of zone 4; their coexpression of α-internexin is consistent with this view. The proximity of their projection sites is also consistent with the proposal that α-internexin plays a spatio-temporally defined role in targeting axons to the OB.

Acknowledgments

This work was supported in part by NIH DC006972, DC00210, DC006291 to CAG and NIH DC006335 to MRA. The authors are indebted to Drs. Helen Treloar and Carrie Iwema for continuing support and guidance and to Ulyana Uboha, Christine Kaliszewski, and Dolores Montoya for outstanding technical assistance. Appreciation is also extended to all members of the Greer Lab for proofreading and generous assistance.

REFERENCES

Akins, MR.; Greer, CA. Catenins define axon paths in the developing mouse olfactory system. 2005. In submission

Ameen NA, Figueroa Y, Salas PJ. Anomalous apical plasma membrane phenotype in CK8-deficient mice indicates a novel role for intermediate filaments in the polarization of simple epithelia. J Cell Sci. 2001; 114:563–575. [PubMed: 11171325]

Astic L, Saucier D. Anatomical mapping of the neuroepithelial projection to the olfactory bulb in the rat. Brain Res Bull. 1986; 16:445–454. [PubMed: 3719376]

Astic L, Saucier D. Topographical projection of the septal organ to the main olfactory bulb in rats: ontogenetic study. Brain Res. 1988; 470:297–303. [PubMed: 2464410]

Astic L, Saucier D, Holley A. Topographical relationships between olfactory receptor cells and glomerular foci in the rat olfactory bulb. Brain Res. 1987; 424:144–152. [PubMed: 2446705]

Au WW, Treloar HB, Greer CA. Sublaminar organization of the mouse olfactory bulb nerve layer. Journal of Comparative Neurology. 2002; 446:68–80. [PubMed: 11920721]

Bastiani MJ, Harrelson AL, Snow PM, Goodman CS. Expression of fasciclin I and II glycoproteins on subsets of axon pathways during neuronal development in the grasshopper. Cell. 1987; 48:745–55. [PubMed: 3545496]

Beil M, Micoulet A, von Wichert G, Paschke S, Walther P, Omary MB, Van Veldhoven PP, Gern U, Wolff-Hieber E, Eggermann J, Waltenberger J, Adler G, Spatz J, Seufferlein T. Sphingosylphosphorylcholine regulates keratin network architecture and visco-elastic properties of human cancer cells. Nat Cell Biol. 2003; 5:803–811. [PubMed: 12942086]

Belecky-Adams T, Holmes M, Shan Y, Tedesco CS, Mascari C, Kaul A, Wight DC, Morris RE, Sussman M, Diamond J, Parysek LM. An intact intermediate filament network is required for

collateral sprouting of small diameter nerve fibers. J Neurosci. 2003; 23:9312–9319. [PubMed: 14561858]

Berghard A, Buck LB. Sensory transduction in vomeronasal neurons: evidence for G alpha o, G alpha i2, and adenylyl cyclase II as major components of a pheromone signaling cascade. J Neurosci. 1996; 16:909–918. [PubMed: 8558259]

Brittis PA, Lu Q, Flanagan JG. Axonal protein synthesis provides a mechanism for localized regulation at an intermediate target. Cell. 2002; 110:223–35. [PubMed: 12150930]

Burton PR. Microtubules of frog olfactory axons: their length and number/axon. Brain Res. 1987; 409:71–78. [PubMed: 3495318]

Burton PR, Paige JL. Polarity of axoplasmic microtubules in the olfactory nerve of the frog. Proc Natl Acad Sci U S A. 1981; 78:3269–3273. [PubMed: 6973153]

Cappello P, Tarozzo G, Benedetto A, Fasolo A. Proliferation and apoptosis in the mouse vomeronasal organ during ontogeny. Neurosci Lett. 1999; 266:37–40. [PubMed: 10336178]

Challacombe JF, Snow DM, Letourneau PC. Dynamic microtubule ends are required for growth cone turning to avoid an inhibitory guidance cue. J Neurosci. 1997; 17:3085–3095. [PubMed: 9096143]

Chien CB, Rosenthal DE, Harris WA, Holt CE. Navigational errors made by growth cones without filopodia in the embryonic Xenopus brain. Neuron. 1993; 11:237–251. [PubMed: 8352941]

Chien CL, Lee TH, Lu KS. Distribution of neuronal intermediate filament proteins in the developing mouse olfactory system. J Neurosci Res. 1998; 54:353–363. [PubMed: 9819140]

Cuschieri A, Bannister LH. Development of olfactory mucosa in mouse - electron-microscopy. Journal of Anatomy. 1975; 119:471–498. [PubMed: 1141050]

Dulac C, Axel R. A novel family of genes encoding putative pheromone receptors in mammals. Cell. 1995; 83:195–206. [PubMed: 7585937]

Dodd J, Morton SB, Karagogeos D, Yamamoto M, Jessell TM. Spatial regulation of axonal glycoprotein expression on subsets of embryonic spinal neurons. Neuron. 1988; 1:105–16. [PubMed: 3272160]

Eyer J, Peterson A. Neurofilament-deficient axons and perikaryal aggregates in viable transgenic mice expressing a neurofilament-beta-galactosidase fusion protein. Neuron. 1994; 12:389–405. [PubMed: 8110465]

Feinstein P, Bozza T, Rodriguez I, Vassalli A, Mombaerts P. Axon guidance of mouse olfactory sensory neurons by odorant receptors and the beta2 adrenergic receptor. Cell. 2004; 117:833–846. [PubMed: 15186782]

Feinstein P, Mombaerts P. A contextual model for axonal sorting into glomeruli in the mouse olfactory system. Cell. 2004; 117:817–831. [PubMed: 15186781]

Fliegner KH, Kaplan MP, Wood TL, Pintar JE, Liem RK. Expression of the gene for the neuronal intermediate filament protein alpha-internexin coincides with the onset of neuronal differentiation in the developing rat nervous system. J Comp Neurol. 1994; 342:161–173. [PubMed: 8201029]

Fuchs E, Cleveland DW. A structural scaffolding of intermediate filaments in health and disease. Science. 1998; 279:514–519. [PubMed: 9438837]

Giacobini P, Benedetto A, Tirindelli R, Fasolo A. Proliferation and migration of receptor neurons in the vomeronasal organ of the adult mouse. Brain Res Dev Brain Res. 2000; 123:33–40.

Giannetti N, Pellier V, Oestreicher AB, Astic L. Immunocytochemical study of the differentiation process of the septal organ of Masera in developing rats. Brain Res Dev Brain Res. 1995; 84:287–293.

Giannetti N, Saucier D, Astic L. Organization of the septal organ projection to the main olfactory bulb in adult and newborn rats. J Comp Neurol. 1992; 323:288–298. [PubMed: 1383286]

Gilbert S, Loranger A, Daigle N, Marceau N. Simple epithelium keratins 8 and 18 provide resistance to Fas-mediated apoptosis. The protection occurs through a receptor-targeting modulation. J Cell Biol. 2001; 154:763–773. [PubMed: 11514590]

Goldstein ME, House SB, Gainer H. NF-L and peripherin immunoreactivities define distinct classes of rat sensory ganglion cells. J Neurosci Res. 1991; 30:92–104. [PubMed: 1795410]

Gorham JD, Ziff EB, Baker H. Differential spatial and temporal expression of two type III intermediate filament proteins in olfactory receptor neurons. Neuron. 1991; 7:485–497. [PubMed: 1910790]

Graziadei PP, Graziadei GA. Neurogenesis and neuron regeneration in the olfactory system of mammals. I. Morphological aspects of differentiation and structural organization of the olfactory sensory neurons. J Neurocytol. 1979; 8:1–18. [PubMed: 438867]

Halpern M, Shapiro LS, Jia C. Differential localization of G proteins in the opossum vomeronasal system. Brain Res. 1995; 677:157–161. [PubMed: 7606461]

Helfand BT, Mendez MG, Pugh J, Delsert C, Goldman RD. A role for intermediate filaments in determining and maintaining the shape of nerve cells. Mol Biol Cell. 2003; 14:5069–5081. [PubMed: 14595112]

Herrada G, Dulac C. A novel family of putative pheromone receptors in mammals with a topographically organized and sexually dimorphic distribution. Cell. 1997; 90:763–773. [PubMed: 9288755]

Hisaoka T, Morikawa Y, Kitamura T, Senba E. Expression of a member of tumor necrosis factor receptor superfamily, TROY, in the developing olfactory system. Glia. 2004; 45:313–324. [PubMed: 14966863]

Inada H, Izawa I, Nishizawa M, Fujita E, Kiyono T, Takahashi T, Momoi T, Inagaki M. Keratin attenuates tumor necrosis factor-induced cytotoxicity through association with TRADD. J Cell Biol. 2001; 155:415–426. [PubMed: 11684708]

Janmey PA, Euteneuer U, Traub P, Schliwa M. Viscoelastic properties of vimentin compared with other filamentous biopolymer networks. J Cell Biol. 1991; 113:155–160. [PubMed: 2007620]

Kaplan MP, Chin SS, Fliegner KH, Liem RK. Alpha-internexin, a novel neuronal intermediate filament protein, precedes the low molecular weight neurofilament protein (NF-L) in the developing rat brain. J Neurosci. 1990; 10:2735–2748. [PubMed: 2201753]

Kasowski HJ, Kim H, Greer CA. Compartmental organization of the olfactory bulb glomerulus. J Comp Neurol. 1999; 407:261–74. [PubMed: 10213094]

Kowalczyk AP, Navarro P, Dejana E, Bornslaeger EA, Green KJ, Kopp DS, Borgwardt JE. VE-cadherin and desmoplakin are assembled into dermal microvascular endothelial intercellular junctions: a pivotal role for plakoglobin in the recruitment of desmoplakin to intercellular junctions. J Cell Sci. 1998; 111(Pt 20):3045–3057. [PubMed: 9739078]

Levavasseur F, Zhu Q, Julien JP. No requirement of alpha-internexin for nervous system development and for radial growth of axons. Brain Res Mol Brain Res. 1999; 69:104–112. [PubMed: 10350642]

Lloyd C, Yu QC, Cheng J, Turksen K, Degenstein L, Hutton E, Fuchs E. The basal keratin network of stratified squamous epithelia: defining K15 function in the absence of K14. J Cell Biol. 1995; 129:1329–1344. [PubMed: 7539810]

Ma L, Yamada S, Wirtz D, Coulombe PA. A ‘hot-spot’ mutation alters the mechanical properties of keratin filament networks. Nat Cell Biol. 2001; 3:503–506. [PubMed: 11331879]

Ma M, Grosmaitre X, Iwema CL, Baker H, Greer CA, Shepherd GM. Olfactory signal transduction in the mouse septal organ. J Neurosci. 2003; 23:317–324. [PubMed: 12514230]

Malnic B, Hirono J, Sato T, Buck LB. Combinatorial receptor codes for odors. Cell. 1999; 96:713–723. [PubMed: 10089886]

Marsh L, Letourneau PC. Growth of neurites without filopodial or lamellipodial activity in the presence of cytochalasin B. J Cell Biol. 1984; 99:2041–2047. [PubMed: 6389568]

Martinez-Marcos A, Jia C, Quan W, Halpern M. Neurogenesis, migration, and apoptosis in the vomeronasal epithelium of adult mice. J Neurobiol. 2005; 63:173–87. [PubMed: 15729685]

Matsunami H, Buck LB. A multigene family encoding a diverse array of putative pheromone receptors in mammals. Cell. 1997; 90:775–784. [PubMed: 9288756]

Mombaerts P, Wang F, Dulac C, Chao SK, Nemes A, Mendelsohn M, Edmondson J, Axel R. Visualizing an olfactory sensory map. Cell. 1996; 87:675–686. [PubMed: 8929536]

Mori K, Nagao H, Yoshihara Y. The olfactory bulb: coding and processing of odor molecule information. Science. 1999; 286:711–715. [PubMed: 10531048]

Ohara O, Gahara Y, Miyake T, Teraoka H, Kitamura T. Neurofilament deficiency in quail caused by nonsense mutation in neurofilament-L gene. J Cell Biol. 1993; 121:387–395. [PubMed: 8468353]

Ressler KJ, Sullivan SL, Buck LB. Information coding in the olfactory system: evidence for a stereotyped and highly organized epitope map in the olfactory bulb. Cell. 1994; 79:1245–1255. [PubMed: 7528109]

Rossler W, Kuduz J, Schurmann FW, Schild D. Aggregation of f-actin in olfactory glomeruli: a common feature of glomeruli across phyla. Chem Senses. 2002; 27:803–810. [PubMed: 12438205]

Runembert I, Queffeulou G, Federici P, Vrtovsnik F, Colucci-Guyon E, Babinet C, Briand P, Trugnan G, Friedlander G, Terzi F. Vimentin affects localization and activity of sodium-glucose cotransporter SGLT1 in membrane rafts. J Cell Sci. 2002; 115:713–724. [PubMed: 11865027]

Ryba NJ, Tirindelli R. A new multigene family of putative pheromone receptors. Neuron. 1997; 19:371–379. [PubMed: 9292726]

Saucier D, Astic L. Analysis of the topographical organization of olfactory epithelium projections in the rat. Brain Res Bull. 1986; 16:455–462. [PubMed: 3719377]

Schwob JE, Farber NB, Gottlieb DI. Neurons of the olfactory epithelium in adult rats contain vimentin. J Neurosci. 1986; 6:208–217. [PubMed: 3944619]

Schwob JE, Youngentob SL, Ring G, Iwema CL, Mezza RC. Reinnervation of the rat olfactory bulb after methyl bromide-induced lesion: timing and extent of reinnervation. J Comp Neurol. 1999; 412:439–457. [PubMed: 10441232]

Shea TB, Beermann ML. Neuronal intermediate filament protein alpha-internexin facilitates axonal neurite elongation in neuroblastoma cells. Cell Motil Cytoskeleton. 1999; 43:322–333. [PubMed: 10423273]

Sin WC, Chen XQ, Leung T, Lim L. RhoA-binding kinase alpha translocation is facilitated by the collapse of the vimentin intermediate filament network. Mol Cell Biol. 1998; 18:6325–6339. [PubMed: 9774649]

St.John JA, Key B. Axon Mis-targeting in the Olfactory Bulb During Regeneration of Olfactory Neuroepithelium. Chem Senses. 2003; 28:773–779. [PubMed: 14654445]

Tian H, Ma M. Molecular organization of the olfactory septal organ. J Neurosci. 2004; 24:8383–8390. [PubMed: 15385621]

Toh BH, Cragg BG, Singh SC, Koh SH. Brain actin demonstrated by immunofluorescence. Exp Neurol. 1978; 58:425–434. [PubMed: 74344]

Toivola DM, Krishnan S, Binder HJ, Singh SK, Omary MB. Keratins modulate colonocyte electrolyte transport via protein mistargeting. J Cell Biol. 2004; 164:911–921. [PubMed: 15007064]

Treloar HB, Feinstein P, Mombaerts P, Greer CA. Specificity of glomerular targeting by olfactory sensory axons. J Neurosci. 2002; 22:2469–2477. [PubMed: 11923411]

Tzivion G, Luo ZJ, Avruch J. Calyculin A-induced vimentin phosphorylation sequesters 14-3-3 and displaces other 14-3-3 partners in vivo. J Biol Chem. 2000; 275:29772–29778. [PubMed: 10887173]

Valiron O, Chevrier V, Usson Y, Breviario F, Job D, Dejana E. Desmoplakin expression and organization at human umbilical vein endothelial cell-to-cell junctions. J Cell Sci. 1996; 109(Pt 8): 2141–2149. [PubMed: 8856510]

Vassar R, Chao SK, Sitcheran R, Nunez JM, Vosshall LB, Axel R. Topographic organization of sensory projections to the olfactory bulb. Cell. 1994; 79:981–991. [PubMed: 8001145]

Verhaagen J, Oestreicher AB, Gispen WH, Margolis FL. The expression of the growth associated protein B50/GAP43 in the olfactory system of neonatal and adult rats. J Neurosci. 1989; 9:683–691. [PubMed: 2918383]

von Campenhausen H, Yoshihara Y, Mori K. OCAM reveals segregated mitral/tufted cell pathways in developing accessory olfactory bulb. Neuroreport. 1997; 8:2607–2612. [PubMed: 9261836]

Wang F, Nemes A, Mendelsohn M, Axel R. Odorant receptors govern the formation of a precise topographic map. Cell. 1998; 93:47–60. [PubMed: 9546391]

Williamson T, Gordon-Weeks PR, Schachner M, Taylor J. Microtubule reorganization is obligatory for growth cone turning. Proc Natl Acad Sci U S A. 1996; 93:15221–15226. [PubMed: 8986791]

Wong P, Colucci-Guyon E, Takahashi K, Gu C, Babinet C, Coulombe PA. Introducing a null mutation in the mouse K6alpha and K6beta genes reveals their essential structural role in the oral mucosa. J Cell Biol. 2000; 150:921–928. [PubMed: 10953016]

Yamada S, Wirtz D, Coulombe PA. Pairwise assembly determines the intrinsic potential for self-organization and mechanical properties of keratin filaments. Mol Biol Cell. 2002; 13:382–391. [PubMed: 11809846]

Yamasaki H, Itakura C, Mizutani M. Hereditary hypotrophic axonopathy with neurofilament deficiency in a mutant strain of the Japanese quail. Acta Neuropathol (Berl). 1991; 82:427–434. [PubMed: 1785256]

Yilmazer-Hanke DM, Hudson R, Distel H. Morphology of developing olfactory axons in the olfactory bulb of the rabbit (Oryctolagus cuniculus): a Golgi study. J Comp Neurol. 2000; 426:68–80. [PubMed: 10980484]

Zhao H, Ivic L, Otaki JM, Hashimoto M, Mikoshiba K, Firestein S. Functional expression of a mammalian odorant receptor. Science. 1998; 279:237–242. [PubMed: 9422698]

Zhu Q, Couillard-Despres S, Julien JP. Delayed maturation of regenerating myelinated axons in mice lacking neurofilaments. Exp Neurol. 1997; 148:299–316. [PubMed: 9398473]

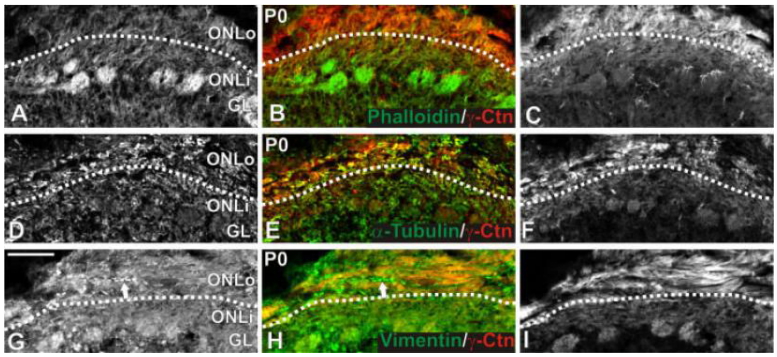

Figure 1.

Localization of microfilaments, microtubules, and vimentin in the P0 ONL. γ-Catenin expression was enriched in the ONLo, allowing identification of the border between ONLo and ONLi (indicated by dotted line). **(A-C)** F-actin localization. Coronal sections were stained for phalloidin (green; A,B) and immunostained for γ-catenin (red; B,C). F-actin was seen uniformly across the ONL and most strongly in glomeruli. **(D-F)** Microtubule localization. Coronal sections were immunostained for α-tubulin (green; D,E) and γ-catenin (red; E,F). α-Tubulin was present ubiquitously within the OB. No difference in expression was seen between the ONLo and ONLi. **(G-I)** Vimentin localization. Coronal sections were immunostained for vimentin (green; G,H) and γ-catenin (red; H,I). Vimentin was expressed by OSN axons as well as non-neuronal tissue (e.g., blood vessel indicated by arrow in G,H). Within OSN axons, expression was uniform across the ONL. Scale bar = 100 μm. Abbreviations: ONLo, outer olfactory nerve layer; ONLi, inner olfactory nerve layer; Ctn, catenin; OSN, olfactory sensory neuron.

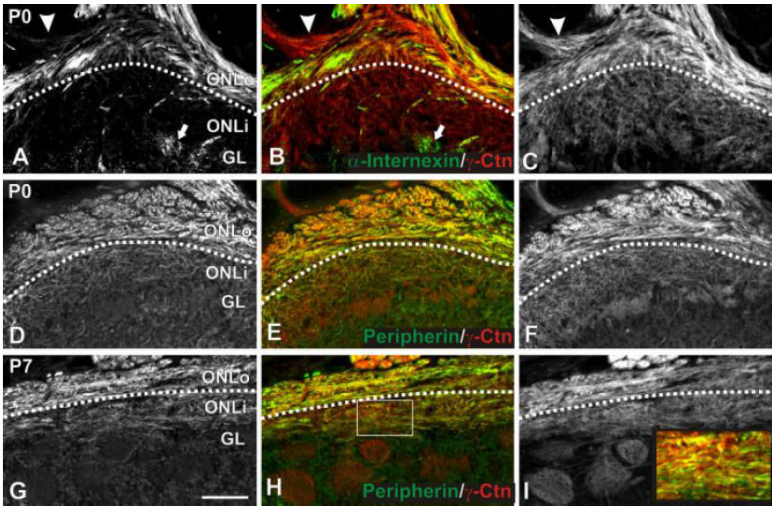

Figure 2.

Localization of α-internexin and peripherin. γ-Catenin expression was used to identify the border between ONLo and ONLi as in Figure 1 for panels A-F. Peripherin expression allowed this distinction in G-I. **(A-C)** α-Internexin localization. Sagittal P0 sections were immunostained for α-internexin (green; A,B) and γ-catenin (red; B,C). α-Internexin was expressed by OSN axons within the ventral ONLo and dendrites within glomeruli in all regions of the OB (arrow in A,B). Expression was seen in only a subset of fascicles within the ONL (e.g., the fascicle indicated by an arrowhead in A,B is negative for α-internexin). **(D-I)** Peripherin localization. P0 **(D-F)** and P7 **(G-I)** coronal sections were immunostained for peripherin (green; D,E,G,H) and γ-catenin (red; E,F,H,I). At P0 (D-F), peripherin was found within OSN axons within the ONLo. Expression was observed in all fascicles. By P7 **(G-I)**, peripherin expression had spread to the ONLi, although staining was more intense within the ONLo. Within the ONLi, staining was heterogeneous (box in H magnified as inset in I). Scale bar = 100 μm. Abbreviations: ONLo, outer olfactory nerve layer; ONLi, inner olfactory nerve layer; Ctn, catenin; OSN, olfactory sensory neuron.

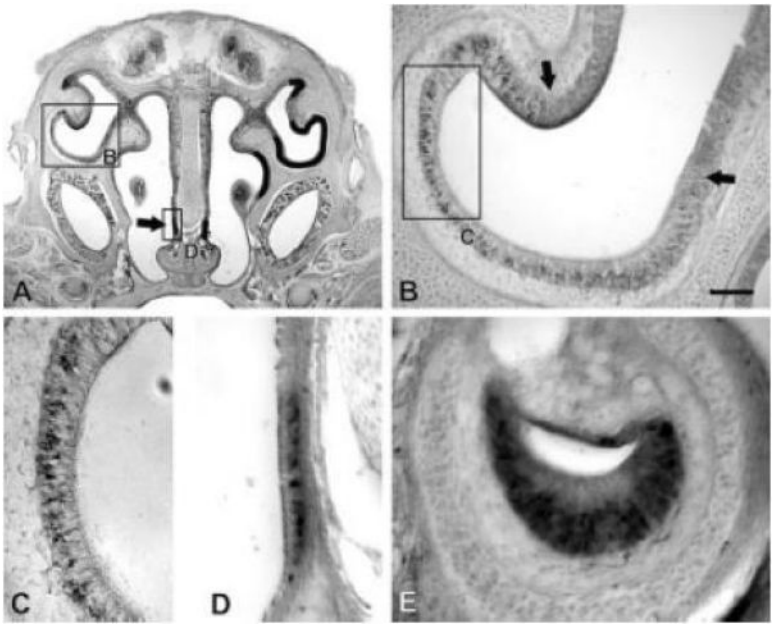

Figure 3.

Localization of cells expressing α-internexin. P0 sections were treated with a probe specific for α-internexin. **(A)** Expression was found in dorsolateral and ventromedial OE as well as in the SO (arrow). Expression is indicated with black lines in the right half of the section. **(B)** An enlargement of the dorsolateral region indicated in A. A sharp border of α-internexin expression was seen (indicated by the arrows). **(C)** An enlargement of the region indicated in B. α-Internexin was expressed by a subset of cells within the basal portion of the OE. **(D)** An expansion of the SO as indicated in A. Expression was seen in a subset of cells in the basal portion of the epithelium. **(E)** Expression within the VNO. α-Internexin was observed by a subset of cells located basally within the epithelium. Scale bar (shown in B) = 500 μm in A; 100 μm in B; 50 μm in C, D, E. Abbreviations: OE, olfactory epithelium; SO, septal organ; VNO, vomeronasal organ.

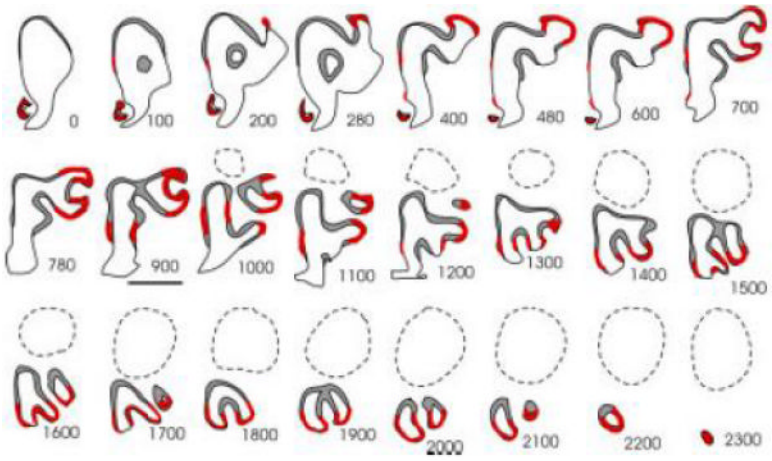

Figure 4.

Summary of α-internexin expression. *In situ* hybridization of coronal P0 sections with a probe specific for α-internexin. Hemisections approximately every 100 μm are summarized in this figure. Presence of expression is indicated by a red line. Expression was seen within the VNO and SO. Additionally, expression was seen within the ventromedial and dorsolateral OE. Caudally, expression was seen ventrally. Scale bar = 1 mm. Abbreviations: OE, olfactory epithelium; SO, septal organ; VNO, vomeronasal organ.

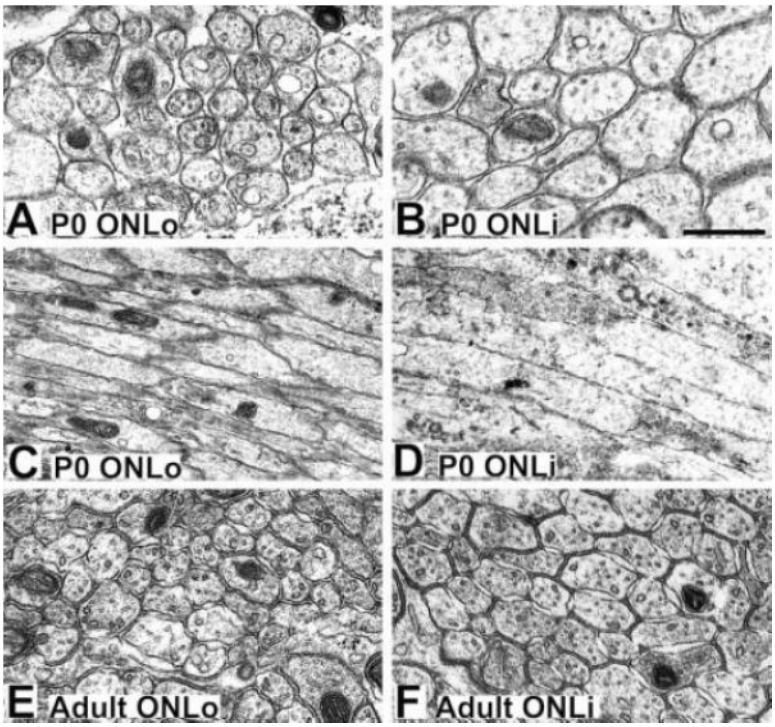

Figure 5.

Electron micrographs of axons in the P0 and adult ONL. **(A,C)** Axons within the P0 ONLo are of roughly uniform diameter. **(B,D)** Axons within the P0 ONLi are larger than those seen in the P0 ONLo. **(E)** Axons within the adult ONLo are approximately the same size seen in the P0 ONLo. **(F)** Axons within the adult ONLi are larger than those in the adult ONLo, but smaller than those in the P0 ONLi. Scale bar = 500 nm in A,B,E,F; 1 μm in C,D. Abbreviations: ONLo, outer olfactory nerve layer; ONLi, inner olfactory nerve layer.

Table 1

Antibodies

Primary antibody	Source, catalog No.	Dilution	Secondary antibody	Dilution
Mouse anti α-internexin	Source: Invitrogen, 32–3600	1:300	Goat anti mouse	1:1,000
	Clone: 2E3		lgG1, Alexa	
	Immunogen: full-length rat α-internexin		488/568	
	Specificity: recognizes α-internexin by immunoblot			
Mouse anti γ-catenin	Source: BD Biosciences, 610254	1:100 w/o antigen retrieval, 1:1000 w/ antigen retrieval	Goat anti-mouse	1:1,000
	Clone: 15		lgG2a, Alexa 488/568	
	Immunogen: human γ-catenin, peptides 553–738			
	Specificity: recognizes γ-catenin by immunoblot			
Mouse anti α-tubulin	Source: Sigma, T5168	1:500	Goat anti-mouse	1:1,000
	Clone: B-5-1-2		lgG1, Alexa	
	Immunogen: sarkosyl-resistant filaments from *Strongylcentrotus* purpuratus (sea urchin) sperm axonemes		488/568	
	Specificity: recognizes α-tubulin by immunoblot			
Rabbit anti peripherin	Source: Chemicon, AB1530	1:300	Donkey anti-rabbit, Alexa	1:1,000
	Immunogen: electrophoretically pure trp-E-peripherin fusion protein, containing all but the 4 N terminal aa of rat peripherin		488/568	
	Specificity: recognizes peripherin by immunoblot			
Mouse anti vimentin	Source: Sigma, V6630	1:3,000	Goat anti-mouse	1:1,000
	Clone: V9		lgG1-Alexa	
	Immunogen: vimentin purified from pig eye lens.		488/568	
	Specificity: recognizes vimentin by immunoblot			